First Insights into PINNs for Accelerating Immune Response Models

Thiago E. Fernandes, Marcelo Lobosco, Rodrigo W. dos Santos

Graduate Program in Computational Modelling
Federal University of Juiz de Fora

July 29, 2024

Introduction

frontiers | Frontiers in Physiology Sections Articles Research Topics Editorial board About journal Subm

A Poroelastic Approach for Modelling Myocardial Oedema in Acute Myocarditis

Wesley de Jesus Lourenço[1] Ruy Freitas Reis[2] Ricardo Ruiz-Baier[3,4,5] Bernardo Martins Rocha[1,2]
Rodrigo Weber dos Santos[1,2] Marcelo Lobosco[1,2*]

[1] Graduate Program on Computational Modelling, Federal University of Juiz de Fora, Juiz de Fora, Brazil
[2] Department of Computer Science, Institute of Exact Sciences, Federal University of Juiz de Fora, Juiz de Fora, Brazil
[3] School of Mathematics and Victorian Heart Institute, Monash University, Melbourne, VIC, Australia
[4] Research Core on Natural and Exact Sciences, Universidad Adventista de Chile, Chillán, Chile
[5] World-Class Research Center "Digital Biodesign and Personalized Healthcare", Sechenov First Moscow State Medical University, Moscow, Russia

Introduction

- In 2017, more than 3 million people were affected by this Myocarditis worldwide, causing about 47,000 deaths [1];
- Simulating the edema formation and its consequences is a costly task;
- In this work we apply Physics Informed Neural Networks (PINN) to adress this issue;

Mathematical model

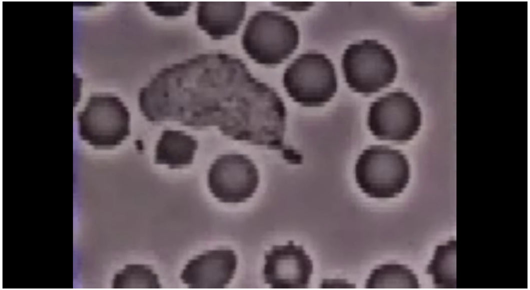

The mathematical model used to describe the pathophysiology of edema formation was proposed in a previous work [1]. This model includes the inflammatory part which describes the interaction between a pathogen and the human immune system.
The pathogen is modelled by:

$$\begin{cases} \frac{d(\phi_f C_b)}{dt} = -r_b + q_b, \; t \in (0,10] \\ C_b(0) = \delta_b, \end{cases} \tag{1}$$

where

$$q_b = c_b C_b \tag{2}$$

$$r_b = \lambda_{nb} C_n C_b \tag{3}$$

Mathematical model

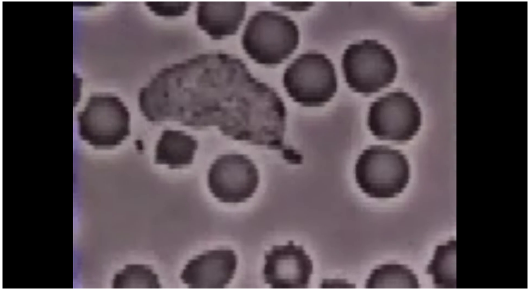

The leukocyte differential model is represented by:

$$\begin{cases} \frac{d(\phi_f C_n)}{dt} = -r_n + q_n, \; t \in (0, 10] \\ C_b(0) = 0 \end{cases} \tag{4}$$

where

$$q_n = \gamma_n C_b (C_{n,max} - C_n) \tag{5}$$

$$r_n = \lambda_{bn} C_n C_b + \mu_n C_n \tag{6}$$

Physics-Informed Neural Networks (PINN)

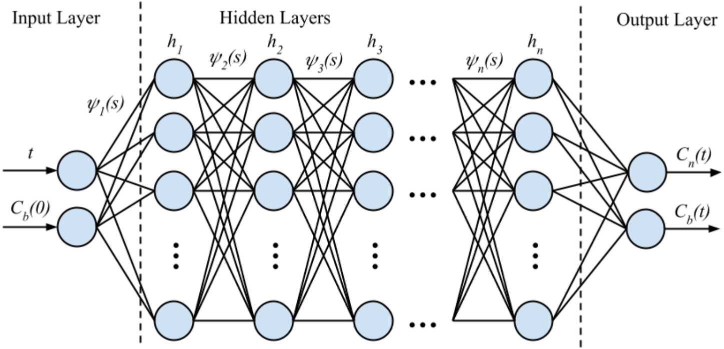

Figure 1: Neural Networks architecture.

Physics-Informed Neural Networks (PINN)

In alignment with the original formulation of Raissi et al. [2], we generally consider PDEs taking the form

$$\frac{\partial u}{\partial t} + \Phi[u] = 0, \; t \in [0, T], \; x \in \Omega \tag{7}$$

subject to the initial and boundary conditions

$$u(0, x) = g(x), \; x \in \Omega \tag{8}$$

$$\beta[u] = 0, \; t \in [0, T], \; x \in \partial\Omega \tag{9}$$

This formulation enables us to define the PDE residuals as follows:

$$\zeta_\theta(t, x) = \frac{\partial u_\theta}{\partial t}(t, x) + \Phi[u_\theta](t, x) \tag{10}$$

PINN architecture grid-search

Consequently, a physics-informed model is trained by minimising the following composite loss function:

$$L(\theta) = L_{ic}(\theta) + L_{bc}(\theta) + L_r(\theta) + L_{dt}(\theta) \tag{11}$$

$$L_{ic}(\theta) = \frac{1}{N_{ic}} \sum_{i=1}^{N_{ic}} \sqrt{(u_\theta(0, x^i_{ic}) - g(x^i_{ic}))^2} \tag{12}$$

$$L_{bc}(\theta) = \frac{1}{N_{bc}} \sum_{i=1}^{N_{bc}} \sqrt{\beta[u_\theta](t^i_{bc}, x^i_{bc})^2} \tag{13}$$

$$L_r(\theta) = \frac{1}{N_r} \sum_{i=1}^{N_r} \sqrt{(\zeta_\theta(t^i_r, x^i_r)^2} \tag{14}$$

$$L_{dt}(\theta) = \frac{1}{N_{dt}} \sum_{i=1}^{N_{dt}} \sqrt{(u_\theta(t^i_{dt}, x^i_{dt}) - u(t^i_{dt}, x^i_{dt}))^2} \tag{15}$$

PINN architecture grid-search

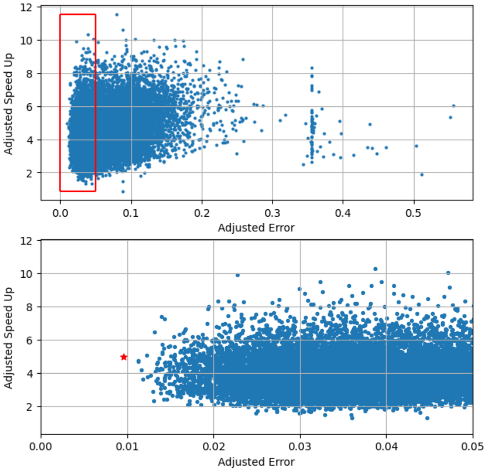

Figure 2: Adjusted error and speed up of the tested architectures.

The adjusted error and speedup are defined respectively by Equations 16 and 17.

$$E_{aj} = RMSE + RSE_{max} \tag{16}$$

$$S_{aj} = \langle S \rangle_{av} - \sigma_s \tag{17}$$

where *RMSE* stands for Root Mean Squared Error and S is the speed up.

PINN architecture grid-search

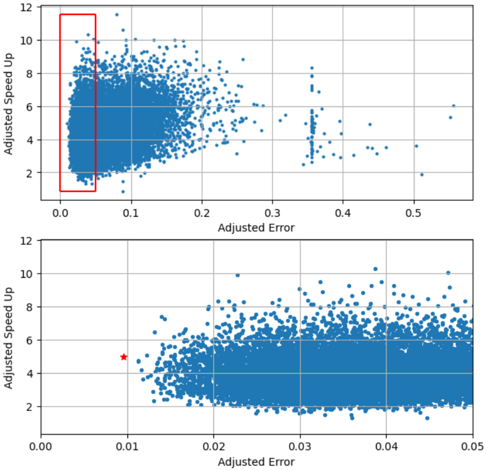

Figure 3: Adjusted error and speed up of the tested architectures.

Considering the 22465 architectures studied, the chosen one is composed by 4 hidden layers with 16, 8, 32, and 16 neurons respectively. Considering the PyTorch documentation, [3], the activation functions are defined as:

$$\psi_1 = \frac{sinh(x)}{cosh(x)} \tag{18}$$

$$\psi_2 = x \cdot \sigma(x) \tag{19}$$

$$\psi_3 = \psi_4 = max(0, x) \tag{20}$$

where x represents the values from the previous layers and $\sigma(x)$ is the logistic sigmoid function.

PINN and NN comparison

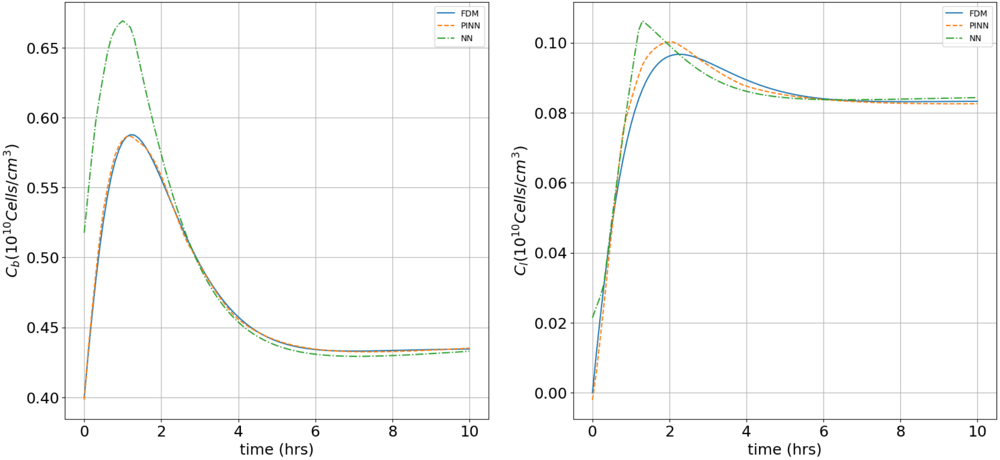

Figure 4: Concentration curves for the different computational models

PINN and NN comparison

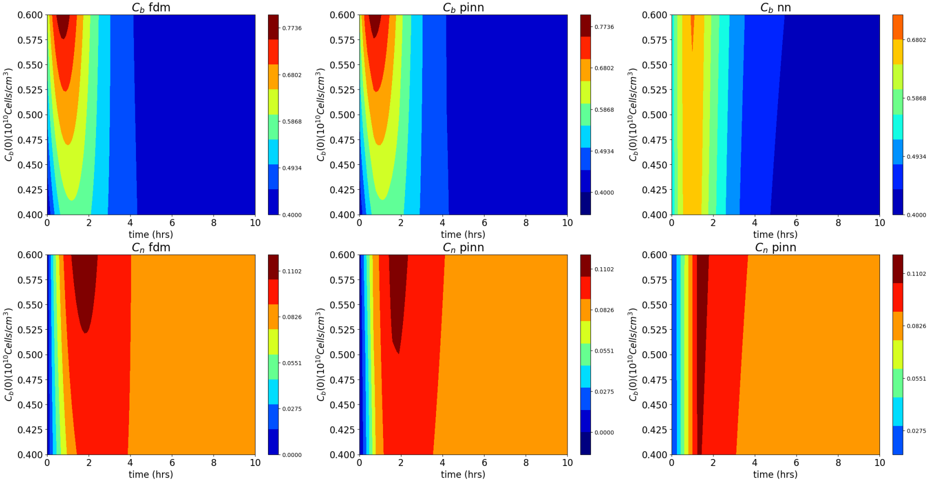

Figure 5: Concentration heat-map for the different computational models

PINN and NN comparison

Table 1 presents the results for the PINN and NN.

Table 1: Experimental results of PINN constrains implementation

Model	RMSE	RSE_{max}	Mean speed up	Speed up Standard Deviation
PINN	0.001530657	0.0080879815	5.93	0.97
NN	0.094564412	0.11761788		

Future Works

- Implement the 2D and 3D models;
- Apply PINNs to the coupled mechanical model;
- Explore the PINN's up-scaling capacities;

[1] W. d. J. Lourenço, R. F. Reis, R. Ruiz-Baier, B. M. Rocha, R. W. Dos Santos, and M. Lobosco, "A poroelastic approach for modelling myocardial oedema in acute myocarditis," *Frontiers in Physiology*, vol. 13, p. 888515, 2022.

[2] M. Raissi, P. Perdikaris, and G. E. Karniadakis, "Physics-informed neural networks: A deep learning framework for solving forward and inverse problems involving nonlinear partial differential equations," *Journal of Computational physics*, vol. 378, pp. 686–707, 2019.

[3] *PyTorch documentation*, PyTorch Foundation, 2023. [Online]. Available: https://pytorch.org/docs/stable/index.html

Thank You